



Geodetic Precession under the Paradigm of a Cosmic Membrane

Stefan Von Weber^{1*} and Alexander Von Eye²

¹Hochschule Furtwangen University, Germany.

²Michigan State University, USA.

Authors' contributions

This work was carried out in collaboration between the both authors. Author SVW designed the study and programmed the computations. Author AVE gave mathematical and physical support. Both authors contributed equally to this work and read and approved the final manuscript.

Article Information

DOI: 10.9734/PSIJ/2016/26365

Editor(s):

- (1) Chao-Qiang Geng, National Center for Theoretical Science, National Tsing Hua University, Hsinchu, Taiwan.
(2) Stefano Moretti, School of Physics & Astronomy, University of Southampton, UK.

Reviewers:

- (1) Luis Acedo Rodríguez, Instituto Univ. de Matemática Multidisciplinar, Universidad Politécnica de Valencia, Valencia, Spain.
(2) Oyvind Gron, Oslo and Akershus University College of Applied Sciences, Norway.
Complete Peer review History: <http://sciencedomain.org/review-history/14928>

Original Research Article

Received 13th April 2016
Accepted 18th May 2016
Published 7th June 2016

ABSTRACT

Cosmic membrane theory (CM) uses the model of a 4-dimensional balloon with a thin skin, expanding in hyperspace. A homogeneous vector field acts perpendicularly from outside on the membrane and causes the gravitation. CM denies the frame-dragging effect of the spin axis of an orbiting gyroscope (also named Lense-Thirring effect). The results of the Gravity Probe B experiment are correct only for geodetic precession. In the case of the frame-dragging effect, data were selected with a particular goal in mind, and only this way they yielded the desired result.

Keywords: Geodetic precession; frame dragging; relativity; membrane; absolute space.

1. INTRODUCTION

One hundred years after the publication of the theory of relativity by Albert Einstein, new scientific insights have been gathered which make it advisable to develop the theory of

relativity further. In this regard, many consider the cosmic background radiation (CBR) by Wilson and Penzias the most important discovery, because CBR depicts, by its dipole character, the absolute motion of Earth in space.

*Corresponding author: E-mail: Stefan.vonWeber@hs-furtwangen.de;

Cosmic Membrane Theory (CM) uses the model of a 4-dimensional balloon with a thin skin, expanding into hyperspace. The 3-dimensional surface of the balloon (the membrane) is our cosmos. A homogeneous vector field acts perpendicularly from outside onto the membrane, and causes the local curvature of the space which is otherwise the cause of gravitation and dark matter. The two major differences between general relativity and CM are: (1) CM denies the frame-dragging effect (also called Lense-Thirring effect), and (2) dark matter is considered to be only a membrane effect that is caused by the interaction of the homogeneous vector field with the curvature and the depth of space. The existence of dark matter cannot be derived from GR. The results of the Gravity Probe B experiment are correct only for the geodetic precession. In the case of the frame-dragging effect, data were selected with a particular goal in mind, and only this way they yielded the desired result.

Despite the criticisms concerning the interpretation the data of the Gravity Probe B experiment, this great, expensive and optimally managed experiment is and remains one of the key experiments of physics and cosmology, comparable to the discovery of nuclear fission by Otto Hahn and Lise Meitner, or the discovery of the cosmic background radiation by Arno Penzias and Robert Wilson. Besides the exact and correct survey of the geodetic precession, the measurements of Everitt, Conklin and their team wear the signature of the membrane.

This article is structured as follows: Section 1 is a brief review of cosmic membrane theory. The theme of section 2 is the change of the speed of light in the gravitational field. Section 3 shows the derivation of the formula of the change of mass in the gravitational field. Section 4 describes the geodetic precession under consideration of an absolute space. Further, we show that the frame-dragging effect is nothing else than the geodetic precession caused by the sun.

2. A BRIEF REVIEW OF COSMIC MEMBRANE THEORY

The prediction of the cosmic micro-wave background radiation by Gamow, Doroshkevich and Novikov [1] and its discovery by Arno Penzias and Robert Wilson [2] with a clearly defined dipole supports the hypothesis of an absolute space (rest inertial system, quantum vacuum, or membrane) in the sense of Newton.

One can explain the dipole as a Doppler-effect that is caused by the motion of the Earth in the rest inertial system. Naturally, this motion is a relative motion in respect to the rest inertial system. That means, whenever we had to deal with clocks or rods we had to consider relativistic effects due to special relativity. Furthermore, nearly all effects caused by the membrane have an adequate translation in the terminology of general relativity. Pioneers are here Dicke and especially Puthoff [3]. The imagination of an absolute space is not far from Mach's principle [4,5,6].

The fundamental element of cosmic membrane theory is the membrane [7,8]. The membrane expands like a balloon in 4-dimensional hyperspace. This membrane is our cosmos. Other names in use are *space-time*, *quantum vacuum*, or *absolute space*. In our 3-dimensional experience world, we are unable to imagine load in the 4th dimension, but we are able to calculate it [9]. We have described the methods of the computation in [8,10], e.g. the construction of the grid and boundary conditions, or the generation of a galactic model. One can find similar methods in [11-13], especially the questions of the range, the use of Gaussian density profiles, complex sequences of steps to find the initial values, or incorporating adaptive mesh refinement and surface tracking.

A disturbance of the membrane appears from the higher dimension and causes a curvature. The disturbance of the cosmic membrane is caused by a homogeneous vector field that acts perpendicularly to the membrane. For properties of the homogeneous vector field see [6,14-15]. One can imagine the vector field as a flow or a radiation or another power source perpendicular to the membrane. The vector field acts only on matter embedded in the membrane, but not on the membrane itself. The curvature caused by the vector field depends on the distribution of matter. The simplest case is that of spherical symmetry. In the case of a 3D-membrane stretched in 4D-space, the vector field acts on a central mass and causes a spherical gravitational funnel in the 4th dimension. Let F_0 be the tension of the undisturbed membrane. It has the dimension of a force per area, i.e. $[N/m^2]$.

We gave in [10] the derivation of the differential equation of the curvature of the 3D-membrane (curvature of space) in the simple case of a central load, with reference to the 2-dimensional analog. We found

$$w'' = -\frac{2w'}{r} \quad (1.1)$$

Each function $w(r)=C_1+C_2/r$ is a solution of the ODE. Differentiation of $w(r) = C_1+C_2/r$ yields $w'(r) = -C_2/r^2$. That is the slope of the membrane at distance r to the center. Let x, y, z be the ordinary spatial coordinates of our coordinate system, and let w be the 4th spatial coordinate, perpendicular to the other coordinates. The w -axis is positioned in the center of the gravitational funnel. If a (small) mass m is situated in the sloped membrane, the vector field causes a force. The decomposition of this force yields the downhill force F_{DH} as

$$F_{DH} = m A_{VF} \sin(\alpha). \quad (1.2)$$

Here, the quantity A_{VF} is the vector-field acceleration, and α is the angle of the slope of the membrane. For small angles is $\sin(\alpha) \approx \tan(\alpha) = w'$. We replace $\sin(\alpha)$ by C/r^2 , and obtain

$$F_{DH} = m A_{VF} w'(r). \quad (1.3)$$

This is Newton's law of gravitation for the case of two masses, i.e., a great central mass that causes the gravitational funnel, and a small mass m . The downhill force F_{DH} is the force of attraction. Now, we apply Eq. (1.3) to the solar system. The quantity R_S is the radius of the Sun, M_S the mass of the Sun, W_{RS} the depth of space w of the deformed membrane at the edge of the Sun, and W'_{RS} is the slope of the membrane at the edge of the Sun. In [7], one can find a series of relations between depth of space, the slope of the membrane at the edge of the Sun, and the gravity. Among others, we find:

$$W'_{RS} = \frac{W_{RS}}{R_S}. \quad (1.4)$$

We can estimate the depth of space W_{RS} at the edge of the Sun using Feynman's radius of excess r_{EX} . We equate formally the radius r_{EX} with the geometrical extension of the path dS from the edge of the Sun to its center [8]. Using Feynman's [9] value of $r_{EX} = dS = 491$ [m] and $R_S = 6.958 \times 10^8$ [m], we obtain the depth of space as $W_{RS} = 1.432 \times 10^6$ [m] or 1432 [km] in our membrane model. The vector-field acceleration A_{VF} is the proportionality factor of the force caused by the homogeneous vector field that acts on one kilogram of matter in the membrane

in direction of the negative 4th dimension. We find [8]:

$$A_{VF} = \frac{g_{RS}}{W'_{RS}} = \frac{g_{RS} R_S}{W_{RS}}. \quad (1.5)$$

Using the ordinary gravitational acceleration of $g_{RS} = 280.1$ [m/s²] at the edge of the Sun, and the above mentioned values of R_S and W_{RS} , we obtain the value of the vector-field acceleration A_{VF} as $A_{VF} = 1.361 \times 10^5$ [m/s²].

The membrane steadies the position of the Sun against the forces of the vector field, just as the elastic mat of a trampoline steadies the weight of an athlete against gravity. The tension F_o of the membrane compensates the action of the vector field. From this, it follows that the force $F_W = M_S A_{VF}$ has to be compensated by the vertical (directed in w -direction) components of the tension F_o that pulls at the surface $4\pi R_S^2$ of the Sun. The vertical component of F_o is $F_{ov} = F_o \sin(\alpha)$. The slope of the membrane is $w' = \tan(\alpha)$. We obtain the equation for the tension of the membrane at the edge of the Sun and for small angles α [8].

$$F_o = \frac{M_S A_{VF}}{4\pi R_S W_{RS}}. \quad (1.6)$$

The numerical value of the tension is $F_o = 2.164 \times 10^{19}$ [N/m²]. Although the membrane is disturbed in the environment of a star, it is still almost flat, considering the tiny slope at the edge of the Sun.

3. SPEED OF LIGHT IN THE GRAVITATIONAL FIELD

The special relativity (SR) of Einstein postulates that light travels with the constant speed c in each inertial system. This does not hold true for accelerated systems, i.e. all systems under the influence of a gravitational field. The idea of a changing speed of light was published already in 1911 by Einstein [16], then by Dicke in 1957. Puthoff [3] developed further Dicke's theory and published in 2002 his "Polarizable-Vacuum approach to GR". This theory is based on the spatial variations of the vacuum electric and magnetic permeabilities. We find in Puthoff's paper, besides the changing speed of light, also the changing of mass under the influence of the gravitational field. Some other authors in the field of changing-speed-of-light theories are [17-19].

In terms of cosmic membrane theory, the speed of light depends on the depth of space, w , and on the properties of the membrane which depend on w [20]. This change in the speed of light is the cause of certain effects, including the bending of light by stars and galaxies, and the Shapiro time delay effect of radar signals with trajectories that graze the edge of the Sun.

The bending of light by stars or galaxies depends on two causes:

1. The common force of attraction of a gravitational field concerning all kinds of matter, including photons;
2. The bending of the wave front of a beam of light because of the different velocities of the beam at the side of the mass and the opposite side.

The more fundamental reason of the second cause is based on the fine structure of the membrane. In agreement with Dicke and Puthoff [3] we showed in [20] that the speed of light changes according to Eq. (2.1) in the case of a gravitational funnel with spherical symmetry.

$$c(r) = c_0 \left(1 - \frac{2a}{r} \right) \quad (2.1)$$

Here, the quantity c_0 is the vacuum speed of light for $r \rightarrow \infty$, and $2a$ is the Schwarzschild radius of the central mass, e.g., the Sun.

4. CHANGE IN MASS IN THE GRAVITATIONAL FIELD

Mass changes in the gravitational field in a way similar to the speed of light. Unfortunately, we have no physical model direct from the membrane to explain this change, but on the one hand we can refer to Puthoff [3], on the other hand we will show that at least one effect is based on this assumption. The square of the kinetic energy, E^2 , is, in agreement with relativity theory,

$$E^2 = (m_{00}c_0^2)^2 + (pc)^2. \quad (3.1)$$

The mass m_{00} is the mass of a body at an infinite distance from the gravitational center and with speed $v=0$ with respect to the surrounding membrane. Velocity c_0 is the speed of light at an infinite distance from the gravitational center. The momentum p is $p=mv_f$. Velocity v_f is the pure rate

of fall of a body falling from the infinite distance to the distance r from the gravitational center. In Eq. (3.2), the quantity K is a constant we still have to determine. We neglect the terms with a^2/r^2 , and obtain the energy E as

$$E = \sqrt{(m_{00}c_0^2)^2 + m_{00}^2 \left(1 + \frac{2Ka}{r} \right) v_f^2 c_0^2 \left(1 - \frac{4a}{r} \right)}. \quad (3.2)$$

We differentiate the energy E with respect to the distance r from the center of gravity. Hereby, we make use of the relations $c(r) = c_0(1 - 2a/r)$, $m(r) \approx m_{00}(1 + Ka/r)$, $v_f^2 = 2GM/r$, $dc/dr = c_0 2a/r^2$, $dm/dr = -m_{00}Ka/r^2$, and $d(v_f^2)/dr = d(2GM/r)/dr = -2GM/r^2$, and neglect the terms with a^2/r^2 . We obtain

$$\frac{dE}{dr} = \frac{m_{00}^2 c_0^2}{2E} \left(-\frac{2GM}{r^2} - \frac{8KaGM}{r^3} + \frac{16GMa}{r^3} \right). \quad (3.3)$$

For the division by E , we rewrite E and neglect again the terms with a^2/r^2 .

$$E = m_{00}c_0^2 \sqrt{1 + \frac{v_f^2}{c_0^2} + \frac{2Kav_f^2}{rc_0^2} - \frac{4av_f^2}{rc_0^2}} \quad (3.4)$$

We insert $v_f^2 = 2GM/r$, and obtain the following expression for the energy E :

$$E = m_{00}c_0^2 \sqrt{1 + \frac{2GM}{rc_0^2} + \frac{4GMKa}{r^2c_0^2} - \frac{8GMa}{r^2c_0^2}}. \quad (3.5)$$

With $a = GM/c_0^2$, and neglecting of all terms with a^2/r^2 and for $r \gg a$, we obtain

$$E = m_{00}c_0^2 \sqrt{1 + \frac{2a}{r} + \frac{4Ka^2}{r^2} - \frac{8a^2}{r^2}} \approx m_{00}c_0^2 \left(1 + \frac{a}{r} \right) \quad (3.6)$$

For small terms behind the 1 (unity) inside the parentheses of Eq. (3.3), the differential quotient dE/dr is then approximately

$$\frac{dE}{dr} = m_{00} \left(-\frac{GM}{r^2} - \frac{4GMKa}{r^3} + \frac{8GMa}{r^3} \right) \left(1 - \frac{a}{r} \right) \quad (3.7)$$

We obtain, after multiplication of the two parentheses and neglecting all terms with a^2/r^2 or

r-terms with a power higher than 3, the following expression:

$$\frac{dE}{dr} = m_{00} \left(-\frac{GM}{r^2} - \frac{4GMKa}{r^3} + \frac{9GMa}{r^3} \right) \quad (3.8)$$

The first term of the right side of Eq. (3.8) is Newton's ordinary gravitation. The second and third terms are relativistic. The action of the homogeneous vector field is the cause of all forces in this case, i.e.

$$\begin{aligned} -\frac{GMm}{r^2} &= -\frac{GM m_{00}(1 + Ka/r)}{r^2} = \\ -\frac{m_{00}GM}{r^2} - \frac{m_{00}GMKa}{r^3} \end{aligned} \quad (3.9)$$

Eq. (3.8) and Eq. (3.9) represent the same force caused by gravity, i.e., we have to equate the second term of the right side of Eq. (3.9) with the second and the third terms of Eq. (3.8). We obtain the new equation

$$-\frac{m_{00}GMKa}{r^3} = (-4K + 9) \frac{m_{00}GMa}{r^3}, \quad (3.10)$$

or $K=4K-9$, or $3K=9$, and from this $K = 3$. The dependency of the mass on the distance r to the central mass, e.g., the Sun, is given by Eq. (3.11) in the case of free fall.

$$m(r) = m_{00} \left(1 + \frac{3a}{r} \right) = m_{00} \left(1 + \frac{a}{r} + \frac{2a}{r} \right) \quad (3.11)$$

Eq. (3.11) is in agreement with Puthoff's "Polarizable-Vacuum approach" [3]. The term a/r is the known relativistic increase of the mass in dependence on velocity. The term $2a/r$ is caused by a change in the properties of the membrane in the gravitational funnel. We have not found a direct derivation of Eq. (3.11) from the supposed properties of the membrane. But this equation receives its justification from the fact that one can compute, with its help, the geodetic precession of an orbiting gyroscope in the gravitational field.

5. GEODETIC PRECESSION AND FRAME-DRAGGING EFFECT

According to general relativity theory, the spin axis of an orbiting gyroscope performs two movements of precession of different magnitude – the geodetic precession and the precession caused by the Lense-Thirring effect (frame dragging). The Lense-Thirring effect should

cause an annual movement of precession of about 39 milliarcseconds (mas) in the west-east direction if the gyroscope moves in a polar orbit with an altitude of 642 km (see Fig. 4.1.1), as in the Gravity Probe B experiment [21]. The geodetic precession appears even for a non-rotating central mass. According to general relativity theory, its annual value is 6606 milliarcseconds (mas) in the orbital direction (cf. the Gravity Probe B experiment [21]).

According to membrane theory:

1. The geodetic precession appears as well, but it generates different intermediate results of earthbound experiments (see, e.g., the Gravity Probe B experiment). The reason for these differences are the motion of the Earth around the Sun and the motion of the Sun in the absolute space. But these motions do not affect the final result of 6600 mas/yr.
2. The Lense-Thirring effect (frame dragging) in the special case of the precession of the spin axis of an orbiting gyroscope appears presumably only if the rotating central mass possesses heterogeneities that cause gravitational waves [22]. In this case, a twisted gravitational field is formed in which the orbital plane of an orbiting gyroscope rotates in free fall. If a rotation appears, then this effect is clearly smaller than the 39 mas/yr of rotation in west-east direction expected in the Gravity Probe B experiment. We expect less than 5% of the above value because of the relatively small heterogeneities of the density of the surface of the Earth, i.e., we expect a maximum rotation of 2 mas/yr.

5.1 Geodetic Precession without Consideration of the Absolute Motion in Space

As mentioned above, one can compute the geodetic precession from the assumptions of membrane theory. If one neglects the motion of the Earth and the Sun in absolute space, one obtains the same value as predicted by general relativity, and the same value that the Gravity Probe B experiment has stated very exactly. The formula of the angular frequency $\dot{\Omega}_G$ of the geodetic precession is, in general relativity,

$$\dot{\Omega}_G = \frac{3GM}{2c^2 r^3} (\vec{r} \times \vec{v}). \quad (4.1.1)$$

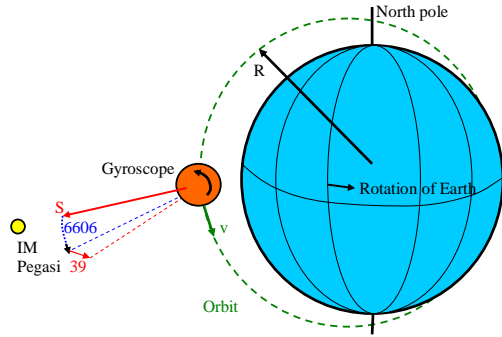


Fig. 4.1.1. Orbiting gyroscope in a polar orbit with geodetic precession of 6606 mas/yr and precession caused by the Lense-Thirring effect of 39 mas/yr

In Fig. 4.1.1, R is the radius center of Earth-orbit, S is the spin vector of the gyroscope, and v is the orbital speed in the polar orbit. As Eq. (4.1.1) shows, the geodetic precession does not depend on the norm of the spin vector S . One finds the direction of the change in the spin, $d\vec{S}$ (here 6606 mas/yr), from the direction of the vector product $\dot{\Omega}_G \times \vec{S}$.

In membrane theory, the main part of the geodetic precession is caused by the decrease of the velocity of waves of any kind in the gravitational funnel [22-23]. We had already presented this effect in Section 3, Eq. (3.1), for the speed of light. The generalization to waves of any kind, i.e., matter waves (de Broglie waves), lends itself in this case, and will be justified by the result [24-25]. Remember, Eq. (3.1) was $c(r)=c_0(1-2a/r)$. This decrease in speed is connected indirectly only with the geometrical curvature of space. The decrease is caused by a change in the inner structure of the membrane [16]. By analogy, we find Eq. (4.1.2).

$$v(r) = v_0 (1 - 2a/r) \quad (4.1.2)$$

Here, v_0 is the velocity of the center of mass of the gyroscope in its orbit, and $2a$ is the Schwarzschild radius of the Earth. An important question is the choice of the correction term $2a/r$ in eq. (4.1.2). Puthoff's "Polarizable-Vacuum approach" [3] would tend primarily to a correction term $3a/r$ as given in eq. (3.11). But the term $3a/r$ leads to another results of the geodetic precession, different to the GR. Therefore we used the term $2a/r$. Another justification is that the term a/r in eq. (3.11) is the known relativistic increase of the mass in dependence on velocity.

Eq. (4.1.2) shows that those parts of the gyroscope move faster that are further away from the Earth. The nearer parts move more slowly. A small brake force appears only when swiveling into orbit. The derivative dv/dr of the speed with respect to distance r from the center of mass has the dimension of an angular frequency, i.e., $1/t$. We find

$$\dot{\Omega}_1 = \frac{dv}{dr} = \frac{v_0 2a}{r^2}. \quad (4.1.3)$$

Using the data of the Gravity Probe B experiment, integration over one year yields the rotation angle $\Omega_1 = 4.283 \times 10^{-5}$ of the spin axis of the gyroscope lying in the plane of the orbit, and the same direction of rotation as the orbit. This angle corresponds to 8834 mas. The angle of 8834 mas is nearly exactly one third greater than the 6606 mas that are predicted for the experiment by general relativity, and has been measured very exactly in the Gravity Probe B experiment. However, the second membrane effect – the increase of the mass in the gravitational funnel – yields the necessary correction of this excessively high value. Together, the two effects yield a rotation angle of 6623 mas. The small deviation from the target value of 6606 mas/yr is caused mostly by imprecise orbital parameters.

Eq. (3.11), $m(r) = m_{00} (1 + a/r + 2a/r)$, of Section 3 describes the change in mass m in the gravitational field of a central mass with the Schwarzschild radius $2a$, at the distance r from the center of the gravitational funnel. Here, the term a/r does not apply. The term $2a/r$ describes the change in mass as a function of the distance r in the gravitational funnel.

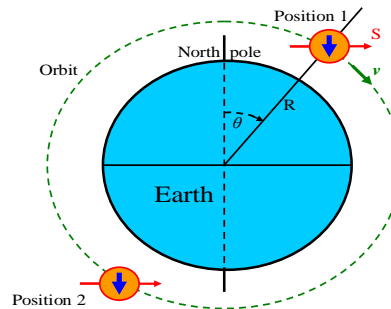


Fig. 4.1.2. The gyroscope in two different positions

Fig. 4.1.2 depicts the gyroscope at his polar orbit in two positions. In position 1, those volume

elements that are at that side of the gyroscope seen by the viewer (the blue arrow) move in the direction of Earth. The radius R and the velocity v are always perpendicular to each another. The distance of a volume element dV of the gyroscope from the center of gravity (center of Earth) is

$$r(\phi, \theta) = R + r_v \sin(\phi) \cos(\theta). \quad (4.1.4)$$

Here, the quantity θ is the rotating angle (polar angle) of the gyroscope (measured from the North Pole), R is the distance of the gyroscope from the center of Earth, r_v is the distance of the volume element dV from the spin axis S of the gyroscope, and ϕ is the rotating angle of the gyroscope (measured from the equatorial plane) around its spin axis S . The term $\cos(\theta)$ describes the influence of the gravitational force from different directions (radii) and its projection at the orbit. We obtain the rotating angle ϕ by the angular frequency ω of the gyroscope and time t as $\phi = \omega t$. We differentiate the change in mass, $m(r) = m_{oo} (1 + 2a/r)$, with respect to the time t , and obtain

$$\frac{dm}{dt} = \frac{dm}{dr} \frac{dr}{d\phi} \frac{d\phi}{dt} = \frac{m_{oo} 2a}{r^2} r_v \cos(\phi) \omega \cos(\theta) \quad (4.1.5)$$

Now, suppose the spherical gyroscope is divided perpendicularly to the spin axis S into slices of thickness δ . Let be ρ the density of the material. The volume element in cylindrical coordinates is $dV = r_v d\phi dr_v \delta$. Assuming a constant orbital speed v , the above-mentioned change in mass per time unit, dm/dt , causes a change in the momentum $F_v = v dm/dt$ with the dimension of a force.

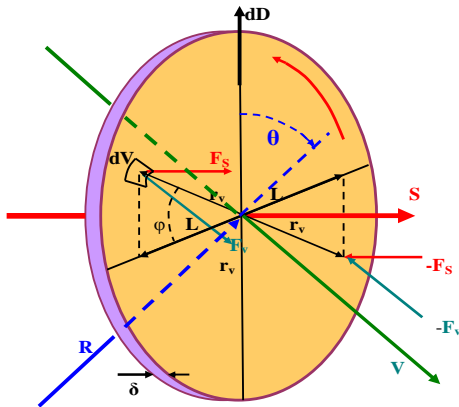


Fig. 4.1.3. Slice of the gyroscope with volume element dV

If the volume element dV is moving toward the Earth, as illustrated in Fig. 4.1.3, i.e., opposite to the radius R , its mass will increase. The force F_v originates in the membrane, and it acts in position 1 of the gyroscope and, for an increasing mass of the volume element dV , in the direction of the orbital velocity v . At the opposite side of the slice, the mass of the mirrored volume element decreases, and the force $-F_v$ acts in the opposite direction of the velocity v . The projections of the two forces, F_v and $-F_v$, at the direction of the spin axis S result in the pair of forces, F_S and $-F_S$, each with the leverage arm L . This pair of forces produces a torque dD of the slice. If the gyroscope is in position 2 (see Fig. 4.1.2), the volume element moves away from Earth, i.e., its mass decreases. The force F_S is directed in the opposite direction of the orbital velocity v . However, velocity has changed its direction after half an orbit around the Earth. That means, the force F_S then has the same direction as in position 1 of the gyroscope. Accordingly, the direction of the force $-F_S$ remains unchanged too at the opposite side of the slice, and, thus, the direction of the torque dD . The torque dD will be zero when the spin axis S and the orbital speed v are perpendicular to each other. This behavior is described mathematically by the once again including factor $\cos(\theta)$ in Eq. (4.1.6).

The velocity v is the orbital speed of the gyroscope around the Earth, the angle $\phi = \omega t$ is the rotating angle of the gyroscope around its spin axis, r_v is the distance of the volume element from the center of the slice, L is the lever arm (it is computed as the projection of the distance r_v at the direction of the vector product $\vec{S} \times d\vec{D}$), F_v is the force acting on the volume element dV , F_S is the projection of F_v at vector S , and δ is the thickness of the slice under consideration. In Fig. 4.1.3, the plane of the orbit is spanned by the vectors v and R . The lever arm L of the torque $L \cdot F_S$ depends on the rotating angle ϕ as $L = r_v \cos(\phi)$. For this reason, the factor $\cos(\phi)$ appears again (i.e., now as factor $\cos^2(\phi)$ in Eq. (4.1.6)). The projection F_S of the force F_v at the direction of the rotating axis S depends on the polar angle θ of the momentary position of the gyroscope at its orbit ($F_S = F_v \cos(\theta)$). For this reason, the factor $\cos(\theta)$ appears again (i.e., now as factor $\cos^2(\theta)$ in Eq. 4.1.6)). We replace the mass m_{oo} in Eq. (3.11) by the mass of the volume element, i.e., $m_{oo} = \rho dV = \rho r_v d\phi dr_v \delta$, and consider the fact that the torque is computed with the couple of forces, F_S and $-F_S$, and the same lever arm L (first factor of 2 in Eq. (4.1.6)). The torque dD acting on the slice is then

$$dD = \frac{2 \cdot v \cdot \rho \cdot \delta \cdot r_V \cdot d\phi \cdot dr_V \cdot 2 \cdot a \cdot \omega \cdot r_V^2 \cdot \cos^2(\phi) \cdot \cos^2(\theta)}{r^2} \quad (4.1.6)$$

We perform the integration in two steps, and only for one half of the slice, because the factor of 2 (mentioned above) is already present in Eq. (4.1.6). Therefore, in the first step of integration, we integrate with respect to the angle ϕ from 0 to π . In the second step of integration, we integrate with respect to the radius r_V , running from the center ($r_V=0$) to the radius r_G ($r_V=r_G$) of the slice of the gyroscope. This way, we get the full torque D acting on the slice. Now, the torque D depends only on the polar angle θ .

$$D = \frac{\pi \cdot 4 \cdot v \cdot \rho \cdot \delta \cdot r_G^4 \cdot a \cdot \omega}{2 \cdot 4 \cdot r^2} \cdot \cos^2(\theta) \quad (4.1.7)$$

The moment of inertia J_S of the slice is $J_S = (\pi \delta \rho r_G^4) / 2$ with respect to its spin axis. If a torque D acts on a spinning gyroscope with angular frequency ω and moment of inertia J_S , and the torque acts perpendicularly to the spin axis of the gyroscope, the precession of the gyroscope is

$$\dot{\Omega}_2 = \frac{D}{J_S \cdot \omega} = \frac{v \cdot a}{r^2} \cos^2(\theta) \cdot \quad (4.1.8)$$

Vector F is the force produced by torque D . The direction of the vector \vec{F} (or of the vector $-\vec{\Omega}$ respectively) is the one given by the vector product $\vec{D} \times \vec{S}$. By centrifugal theory, the direction of the change $d\vec{S}_2$ of the spin is given by the vector product $\vec{S} \times \vec{F}$, i.e., the opposite direction of the main effect of $\dot{\Omega}_1$ in Eq. (4.1.3). However, the precession $\dot{\Omega}_2$ still depends on the polar angle θ . Integration of $\dot{\Omega}_2$ with respect to the polar angle θ from 0 to 2π produces the factor $1/2$, i.e.

$$\dot{\Omega}_2 = \frac{D}{J_S \cdot \omega} = \frac{v \cdot a}{2r^2} \cdot \quad (4.1.9)$$

Under consideration of the opposite signs, the two equations (4.1.3) and (4.1.9) result in Eq. (4.1.1). That means, the result is the same as given by general relativity. The error bars given in the final report of Everitt et al. [21] are 6601.8 ± 18.3 mas/yr. Our own numerical integration of eq. (4.1.1) yielded a value of 6623

mas/yr. The t-value of $t = (6623 - 6601.8) / 18.3 = 1.25$ results in an error probability of 25% for the rejection of the null hypothesis. That means our result is within the error bars of the GPB experiment. The discrepancy to the prediction of the GR with 6606.1 mas/yr is simply a consequence of our imprecise knowledge of the exact orbital parameters of the GPB experiment.

5.2 Geodetic Precession under Consideration of Absolute Motion in Space

In membrane theory, Eq. (4.1.1) is only a partial result. The true speed v of the gyroscope in the rest inertial system is composed as vector sum of the orbital speed $v_G = 7.6$ km/s of the gyroscope in its polar orbit around the Earth, the speed $v_E = 30$ km/s of the Earth during its orbit around the Sun, and the speed $v_S = 369$ km/s of the Sun in the absolute space in direction of the constellation Virgo.

The guide star IM Pegasi was the target in the Gravity Probe B experiment. Seen from the Sun, it is located in about the direction opposite to the constellation Virgo. The Sun moves with a speed of 369 km/s in the direction of this constellation (see Fig. 4.2.1).

In the equatorial coordinate system, IM Pegasi has the coordinates right ascension 22h 53m, declination $+16^\circ 50'$. The Virgo cluster has the coordinates right ascension 12h 27m, declination $+12^\circ 43'$. If we arrange the x-axis of our coordinate system so that it is directed to the guide star IM Pegasi, then the Sun moves in the xy plane on a trajectory through the absolute space at an angle of 10h 26m or $\beta_{SX} = -156.5^\circ$ (or $+203.5^\circ$ respectively) to the x-axis. Because of the positive declinations of $+16^\circ 50'$ of the guide star and $+12^\circ 43'$ of the Virgo cluster, the trajectory of the Sun in the xz plane has an angle $\beta_{SZ} = 60.5^\circ$ with the z-axis. Because of the declination of the x-axis, the z-axis of our coordinate system is not perpendicular to the plane of the celestial equator, but it is slanted by $16^\circ 50'$ in direction of the Virgo cluster. The y-axis of our coordinate system points away from the viewer backward, and it is lying in the plane of the celestial equator.

On March 21, the Sun is positioned in the constellation Ram (spring point and zero point of the astronomical measurement of the angle of the right ascension in the plane of the celestial equator). Neglecting small angles, the

x-component v_x of the speed v of the gyroscope in the absolute space is

$$v_x = v_S \cos(\beta_{SX}) - v_E \sin(\alpha_E) + v_G \cos(\theta_G) \quad (4.2.1)$$

and the z-component v_z is

$$v_z = v_S \cos(\beta_{SZ}) - v_G \sin(\theta_G). \quad (4.2.2)$$

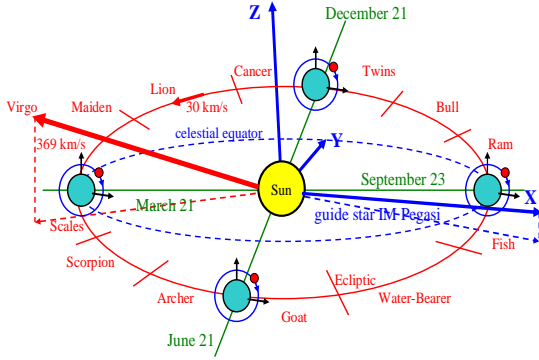


Fig. 4.2.1. The orbit of the earth on the ecliptic with the zodiac

Here, the y-component, v_y , is neglected. In Eq. (4.2.1), the angle α_E is the orbital angle of the Earth around the Sun (here measured from the x-axis), and θ_G is the orbital angle of the gyroscope on its polar orbit. Our x-axis is positioned in the plane of the orbit. The angle θ_G is measured from the z-axis. Now, we show that Eq. (4.1.1) remains valid even in absolute space. If the vectors \vec{r} and \vec{v} are not perpendicular to each other then $\vec{r} \times \vec{v} = r v \sin(\alpha_{rv})$ holds, where the quantity α_{rv} is the angle between the vectors \vec{r} and \vec{v} . Eq. (4.1.2) changes to be $v(r) = v_0(1 - 2a/r) \sin(\alpha_{rv})$. The velocity v_0 is the absolute velocity in the orbital plane. The Eq. (4.1.3) becomes the Eq. (4.2.3).

$$\dot{\Omega}_1 = \frac{dv}{dr} = \frac{v_0 2a \sin(\alpha_{rv})}{r^2}. \quad (4.2.3)$$

As Eq. (4.2.3) states, the projection F_S of the force F_v onto the direction of the spin axis S does not further depend directly and exclusively on the polar angle θ_G of the orbit of the gyroscope, but on the angle α_{vS} , i.e., the angle between speed \vec{v} and spin axis \vec{S} in the xz plane. The tangent of the angle α_{vS} is $\tan(\alpha_{vS}) = v_z/v_x$ and thereby $\alpha_{vS} = \arctan(v_z/v_x)$. The term $\cos(\theta_G)$ is, as before, part of the description of the distance of the

volume element dV of the gyroscope from the center of gravitation (center of Earth). Thereby, Eq. (4.1.7) transforms into Eq. (4.2.4).

$$D = \frac{\pi \cdot 4 \cdot v \cdot \rho \cdot \delta \cdot r_G^4 \cdot a \cdot \omega}{2 \cdot 4 \cdot r^2} \cdot \cos(\theta_G) \cos(\alpha_{vS}), \quad (4.2.4)$$

and Eq. (4.1.8) transforms into Eq. (4.2.5).

$$\dot{\Omega}_2 = \frac{v \cdot a}{r^2} \cos(\theta_G) \cos(\alpha_{vS}). \quad (4.2.5)$$

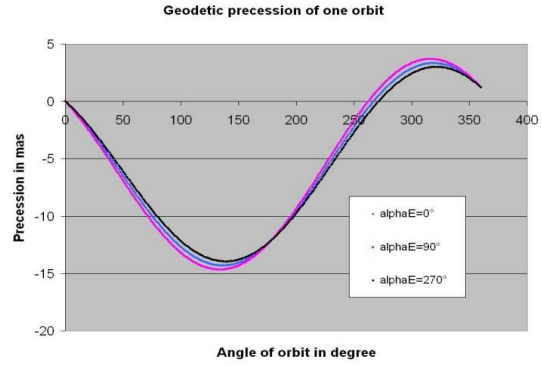


Fig. 4.2.2. Geodetic precession of one orbit of the gyroscope for three different positions of the earth

The system of the Eq. (4.2.3) to Eq. (4.2.5) was integrated numerically. Fig. 4.2.2 depicts the precession $\Omega(\alpha_G)$ as a function of the orbital angle α_G of the gyroscope for three different angles α_E , i.e., for three different positions of the Earth on its orbit around the Sun. The curves for the angles $\alpha_E=0^\circ$ and $\alpha_E=180^\circ$ do not differ. The geodetic precession Ω increases by 1.228 mas during each orbit, which sums to a total angle of 6623 mas for 5394 orbits during one year, i.e., nearly exactly the value of $6601,8 \pm 18,3$ mas/yr given by Everitt et al. [21]. The prediction based on general relativity is 6606.1 mas/yr.

5.3 Geodetic Precession Caused by the Gravity of the Sun versus Frame Dragging

Everitt et al. [21] specify the influence of the gravity of the Sun as a west-east precession of 16 mas/yr, i.e., the same direction as the expected frame dragging effect (Lense-Thirring effect). Everitt et al. adjust their frame dragging value by this value of 16 mas, but also by several other known influences, e.g., the motion of the guide star IM Pegasi. The Earth orbits the ecliptic

once every year. On March 21, the Sun resides, seen from the Earth, at the First Point of Aries (constellation Ram), the Earth, seen from the Sun, at the First Point of Libra (constellation Scales). From this point on, the Sun moves in direction of the constellation Scorpion (see Fig. 4.2.1). The plane of the celestial equator and the plane of the ecliptic are inclined against each other by an angle of 23.5°. The line of intersection runs between the First Point of Aries and the First Point of Libra. We take the line of intersection to be our x-axis directed to the First Point of Aries. The y-axis lies in the plane of the ecliptic and is directed to the constellation Cancer. The z-axis (rotation axis) is perpendicular to the ecliptic and points in the same direction as $\vec{x} \times \vec{y}$. Neglecting small angles, the Sun moves on a trajectory through the absolute space in the direction of the Virgo cluster. The trajectory has an angle of 12 h 27 m or $\alpha_{Virg}=186.75^\circ$ with our x-axis lying in the xy plane (the dashed red line in Fig. 4.2.1). The angle $\beta_{SZ}=60.5^\circ$ of the trajectory with the z-axis in the xz plane remains nearly unchanged because of the positive declination of the guide star IM Pegasi (about $\delta_{Peg}=17^\circ$) and the positive declination of Virgo cluster (about $\delta_{Virg}=13^\circ$). The term $\cos(\delta_{Peg})$ appears because of the declination of IM Pegasi. The formulas from Section 4.2 remain nearly unchanged. Eq. (4.2.1) transforms to Eq. (4.3.1).

$$\dot{\Omega}_1 = \frac{dv}{dr} = \frac{v_0 2a \sin(\alpha_{rv})}{r^2} \cos(\delta_{Peg}). \quad (4.3.1)$$

Here, the radius r is the mean Sun-Earth distance, and $2a$ is the Schwarzschild radius of the Sun. If we compute the correction term $\dot{\Omega}_2$ for Eq. (4.3.1), the projection F_S of force F_V onto the spin axis S does not further depend directly and exclusively on the orbital angle α_E of the Earth, but on the angle α_{vS} , the angle between the speed \vec{v} of the Earth and spin axis \vec{S} lying in the xy plane. Under consideration of this change in the meaning of the angle α_{vS} , Eq. (4.2.5) in Section (4.2) stays nearly unchanged, too. However, we have to replace the orbital angle θ_G of the gyroscope by the orbital angle α_E of the Earth. Because of the fact that, for $\alpha_E=0$, already a small angular deviation of $\alpha_{Peg}=-17^\circ$ exists between the orbital angle α_E of the Earth and the spin vector \vec{S} of the gyroscope, we now take into account this deviation. For $\alpha_E = -\alpha_{Peg}$, the radius and the projection of the translational

motion of the gyroscope are perpendicular to each other, and, therefore, contribute no component in the direction of the radius. This behavior is described mathematically by the term $\cos(\alpha_E + \pi/2 - \alpha_{Peg})$. The term $\cos(\delta_{Peg})$ is needed because of the declination of the guide star IM Pegasi. We find Eq. (4.3.2) for the correction term.

$$\dot{\Omega}_2 = \frac{v \cdot a}{r^2} \cos(\alpha_E + \pi/2 - \alpha_{Peg}) \cos(\alpha_{vS}) \cos(\delta_{Peg}). \quad (4.3.2)$$

Neglecting small angular deviations, the x-component v_x and the y-component v_y of the orbital speed \vec{v} of the Earth in absolute space are

$$v_x = v_S \cos(\alpha_{Virg}) \cos(\delta_{Virg}) - v_E \sin(\alpha_E), \quad (4.3.3)$$

$$v_y = v_S \sin(\alpha_{Virg}) \cos(\delta_{Virg}) + v_E \cos(\alpha_E). \quad (4.3.4)$$

The angle α_{vS} is

$$\alpha_{vS} = \arctan(v_y/v_x) + \alpha_{Peg}. \quad (4.3.5)$$

The angle α_{Peg} is the right ascension of the guide star IM Pegasi of 22 h 53 m ($\alpha_{Peg} = -17^\circ$). The system of Eq. (4.3.2) to Eq. (4.3.5) was integrated numerically. Fig. 4.3.1 depicts the precession Ω_{WO} for two orbits of the Earth on its trajectory around the Sun.

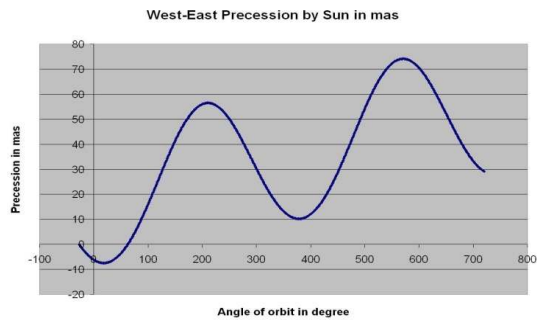


Fig. 4.3.1. Geodetic west-east precession of Earth, caused by the gravitation of the Sun, for two years

The angle Ω_{WO} of precession increases by about 18 mas per year, which is in good agreement with general relativity. In addition, a strong sine-shaped deviation arises from the straight line. The cause for this deviation is the motion of the

Sun and, therefore, also that of the Earth. One can separate the two parts of the curve in Fig. 4.3.1 using a nonlinear regression analysis resulting in a straight line and a sine wave. The model of the regression is

$$\Omega(\alpha_E) = b_0 + b_1\alpha_E + b_2 \sin(\alpha_E - \phi). \quad (4.3.6)$$

The OLS estimates of the regression coefficients are $b_0=18.87$, $b_1=0.0462$, $b_2=27.64$, and $\phi=115.3^\circ$. The increase per year is 17.9 mas, a value which is close to the value of 19 mas given by general relativity. The reason of choosing the range of the orbital angle of the Earth, i.e. α_E runs from -22° to 341° , depends, on the one hand, on the definition of the x-axis, and, on the other hand, on the fact that, in the Gravity Probe B experiment (which we refer to) the data have been collected within the period of one year starting on September 1.

The frame-dragging effect (Lense-Thirring effect) does not appear in the present state of our membrane theory. The reason of our opinion is that, for the rotating Earth, the gravitational funnel is nearly smooth and without a dragging property. On the other hand, the results of the LAGEOS laser ranging experiments and its follower experiments state a clear precession of the orbital plane of the polar orbit as described by Ciufolini [26]. But there is a difference between the LAGEOS experiments and the Gravity Probe B. In the LAGEOS experiments the orbital plane performs a precession as a whole. In the GPB experiment the spin axis of the gyroscope performs (or should perform) the precession. We suppose that this difference has some deeper physical meaning. Therefore, we restrict our critics of the GPB experiment in this article to the precession of a spin axis of an orbiting gyroscope. Due to our calculations, we assert that at least 95% of the results of the Gravity Probe B experiment which refers to the frame-dragging effect, can be considered a misinterpretation of confusing data. The main cause of the misinterpretation is the negation of the absolute motion of Earth and Sun in space.

When the central mass is not cylindrically symmetric, but it has heterogeneities on the surface (e.g., the mountains and oceans on the surface of the Earth) or in the inside, perturbations of the gravitational field propagate with the speed of light with the shape of a spiral. These perturbations could possibly cause a weak

Lense-Thirring effect, but we have not found any evidence for this effect.

Of course, we have reflected on the way the authors of the Gravity Probe B reports [21,27] arrived at their result of 37.2 ± 7.2 mas/yr for the frame-dragging effect. Fortunately, Conklin [27] gave us an indication in his preliminary report in 2008: *"The results from the 85-day analysis is -6632±43 marcs/yr in the North-South direction and -82±13 marcs/yr in the West-East direction using the SQUID and telescope noises. These estimates are consistent with the GR prediction of -6571±1 marcs/yr and -75±1 marcs/yr in the North-South and West-East directions respectively"*.

This means, the estimation of the value of the full year was performed using mostly the data of the period between December 12, 2004 and March 4, 2005, i.e., using the data of 85 days (also a period of only 45 days has been mentioned, i.e., from January 1, 2005 to February 15, 2005). The two periods are 23%, or 12% respectively, of the full year. Had we used the data of the 85 days period as seen in Fig. 4.3.1, we would have computed a value for the west-east precession that is much too large. The reason for this over-estimation is that the above-mentioned 85 days period lies in the angular sector of 80° to 163° of the orbital angle α_E of the orbit of the Earth. In this sector, the curve has a strong, nearly linear, positive slope.

However, if one tries and computes a regression line $\Omega(\alpha_E) = b_1\alpha_E$ with the data of the first full year of Fig. 4.3.1, which yields the regression coefficient $b_1=0.1585$, the sine wave will be intersected asymmetrically. Fig. 4.3.2 depicts the result.

Now, one computes the residuals $R(\alpha_E) = \Omega(\alpha_E) - b_1\alpha_E$, and then, with the residuals, the regression line $S(\alpha_E) = b_{2S} \sin(\alpha_E - \phi_S)$, which yields the regression coefficients $b_{2S}=20.45$ and $\phi_S=93^\circ$. This way, the new regression coefficient of the sine is smaller than the coefficient of the combined regression model of Eq. (4.3.7), i.e., $b_{2S}=20.45$ instead of $b_2=27.64$. We eliminate the thus estimated part of the sine wave in the data of the curve in Fig. 4.3.2, and obtain the result depicted in Fig. 4.3.3.

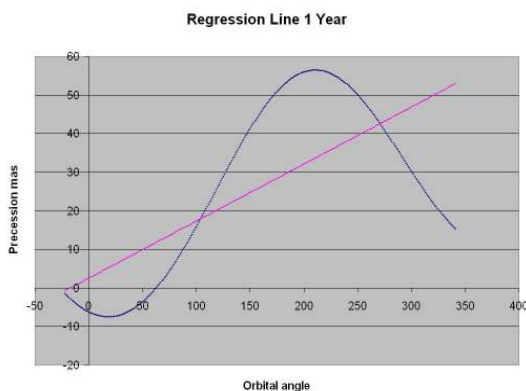


Fig. 4.3.2. Regression line and sine wave intersected asymmetrically

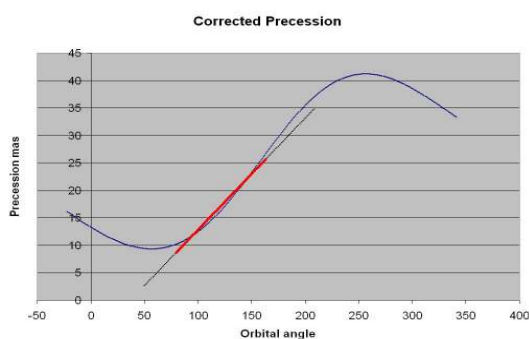


Fig. 4.3.3. West-east precession with partially reduced sine

The red part of the linear trend in Fig. 4.3.3 lies within the 85 days period of December 12, 2004, to March 4, 2005. The slope of $b_1=0.2033$ yields a value for the full year of $\Omega=73.2$ mas/yr (in the case of the 45 days period a value of $\Omega=76.3$ mas/yr). Conklin's first estimation of $\Omega=82\pm 13$ mas/yr changed by further analyses in the final report of Everitt [21] to $\Omega=73.4$ mas/yr (thereof 37.2 mas/yr for the targeted frame-dragging effect, 16.2 mas/yr for the relativistic geodetic effect of the Sun, and 20.0 mas/yr for the proper motion of the guide star IM Pegasi). Our estimation of $\Omega=73.2$ mas/yr in the case of the 85 days period meets nearly exactly Everitt's value of $\Omega=73.4$ mas/yr. This match suggests the conclusion that our approach to data analysis accords with the approach taken by the data analysts of the Gravity Probe B experiment.

Despite our criticism of the selective interpretation of the data of the Gravity Probe B experiment, this great, expensive and optimally performed experiment is one of the key

experiments in modern physics and cosmology, comparable to the discovery of the atomic fission by Otto Hahn and Lise Meitner, or the discovery of the cosmic microwave background radiation by Arno Penzias and Robert Wilson. In addition to the exact verification of the geodetic precession, the measurements of Everitt, Conklin and their team bear the signature of the membrane. We are still unable to estimate the scientific value of this discovery today.

6. RESULTS AND DISCUSSION

One important difference between general relativity and CM is that the cosmic membrane theory does not need the frame-dragging effect (also called Lense-Thirring effect). For a spinning mass of cylindrical symmetry, we will not find a twisted gravitational field, and, therefore, also no frame-dragging. Only when the spinning mass has heterogeneities, a twisted gravitational field will be generated that could be the cause of this effect. If this effect actually exists, it should be significantly smaller than predicted by Lense and Thirring. Here we are in a clear contradiction to the results of the LAGEOS mission (compare Ciufolini [27]). That means further research for the CM model. Otherwise, the LAGEOS experiments measured the precession of the orbital plane of the satellite, and not the precession of the spin axis, as performed in the GBP experiment. Here, Everitt and Conklin have not included the influence of the motion of the Sun and the Earth in the analysis of the Gravity Probe B data. They interpreted the relevant measurements as errors. In the case of geodetic precession, the influence of the motion of the Sun and the Earth in the absolute space is marginal. According to the excellent measuring technique of the Gravity Probe B experiment, the conformity of the predictions of the general theory of relativity to the geodetic precession is very strong.

However, we have another case when trying to verify frame-dragging. The only significant gyroscopic effect in west-east direction is the geodetic precession caused by the gravity of the Sun. But this effect is superposed by a strong sine. The cause is the motion of the Sun and the additional motion of the Earth. Everitt and Conklin have erroneously interpreted the slope of the sine curve in an 85-days period as frame-dragging effect.

Despite our criticisms of the interpretation of the data of the Gravity Probe B experiment, this

great, expensive and optimally managed experiment is and remains one of the key experiments in modern physics. Besides the exact and correct survey of the geodetic precession, the measurements of Everitt, Conklin and their team wear the signature of the membrane (the absolute space). Today, this discovery cannot be valued high enough.

A second difference between the cosmic membrane theory and the general theory of relativity concerns the interpretation of dark matter. The general theory of relativity makes no contribution to this issue. In contrast, the cosmic membrane theory posits that dark matter is an effect of the membrane that is caused by the interaction of the curvature and depth of space with the homogeneous vector field. Numerical computations suggest that this idea is fertile.

7. CONCLUSIONS

The cosmic membrane theory and the general relativity are very similar to one another. One can explain nearly all known effects in the same or a similar manner and with the same results. One finds differences in the use of the time. The CM theory uses four spatial coordinates, not three spatial coordinates together with the construct "ct", as GR does. However, by Puthoff's "Polarizable-Vacuum approach to GR" we find a connection between CM and GR.

The frame-dragging effect is, besides the dark matter issue, one point of our special interest. The LAGEOS missions showed with good precision the precession of the orbital planes of the satellites. Otherwise, our calculations in section 4 show that the west-east precession of the spin axis of an orbiting gyroscope is probably caused only by the gyroscopic effect of the Sun. This is a real conflict. Therefore, further research should concentrate on this issue.

- Is the issue a problem of the cosmic membrane theory?
- Is the issue a problem of the general relativity?
- Is the different behavior of an orbiting satellite and an orbiting gyroscope a real fact? In this case we have to revise both theories.

Since the CM theory yields also some interesting contributions to the dark-matter problem, we should pursue all directions and thoughts.

COMPETING INTERESTS

Authors have declared that no competing interests exist.

REFERENCES

1. Naselsky P, Novikov D, Novikov I. The physics of cosmic microwave background. Cambridge University Press; 2006.
2. Penzias AA, Wilson RW. A measurement of excess antenna temperature at 4080 Mc/s, ApJ. 1965;142:419-421. Available:<http://dx.doi.org/10.1086/148307>
3. Puthoff HE. Polarizable-vacuum approach to GR, Found. of Physics. 2002;32:6. Available:<https://arxiv.org/ftp/gr-qc/papers/9909/9909037.pdf>
4. Dunsby PKS, Luongo O. On the theory and applications of modern cosmography. Int. J. Geom. Methods Mod. Phys; 2015. Available: [arXiv:1511.06532 \[gr-qc\]](http://arxiv.org/abs/1511.06532)
5. Hinshaw G, et al. Five-year Wilkinson microwave anisotropy probe (WMAP1); 2008. Available: <http://arxiv.org/abs/0803.0547v2>
6. Kogut A, et al. Dipole anisotropy in the COBE differential microwave radiometers first-year sky maps. Astrophysical Journal. 1993;419:1-6. Available:<http://arxiv.org/abs/astro-ph/9312056>
7. Thorne, Kip S, Price RH, Macdonald DA, (eds.). Black Holes: The membrane paradigm. Yale University Press; 1986.
8. Weber S. von, von Eye A. Monte Carlo study of vector field-induced dark matter in a spiral galaxy. InterStat; 2011. Available:<http://interstat.statjournals.net/YEAR/2011/articles/1108002.pdf>
9. Feynman/Leighton/Sands: Feynman - Vorlesungen über Physik, Oldenbourg Verlag; 1987.
10. Weber S. von, von Eye A. Multiple weighted regression analysis of the curvature of a 3D Brane in a 4D Bulk Space under a Homogeneous Vector Field, InterStat; 2010. Available:<http://interstat.statjournals.net/YEAR/2010/articles/1007003.pdf>
11. Bode T, Haas R, Bogdanovic T, Laguna P, Shoemaker D. Relativistic mergers of supermassive black holes and their electromagnetic signatures. Astrophys. J. 2010;715:1117-1131. Available: [arXiv:0912.0087](http://arxiv.org/abs/0912.0087)

12. Buchman LT, Pfeiffer H, Scheel MA, Szilágyi B. Simulations of non-equal mass black hole binaries with spectral methods, Phys. Rev. Lett. D. 2012;86:1-21. Available: [arXiv:1206.3015](https://arxiv.org/abs/1206.3015)
13. Mösta P, Andersson L, Metzger J, Szilágyi B, Winicour J. The merger of small and large black holes, submitted to class. Quantum. Grav; 2015. Available: arxiv.org/abs/1501.05358
14. Ford LH. Inflation driven by a vector field. Phys. Rev. D. 1989;40:967-972. Available: <http://www.ncbi.nlm.nih.gov/pubmed/10011903>
15. Gogberashvili M. Brane gravity from bulk vector field. Phys. Lett. B. 2003;553:284-288. Available: <http://www.sciencedirect.com/science/article/pii/S0370269302032082>
16. Einstein A. On the Influence of gravitation on the propagation of light. Annalen der Physik. 1911;35:898-908. Available: <https://www.relativitycalculator.com/pdfs/O....LightEnglish.pdf>
17. Bruckman W, Esteban EP. An alternative calculation of light bending and time delay by a gravitational field. Am. J. Phys. 1993;61(8):750. Available: <http://dx.doi.org/10.1119/1.1715>
18. Ellis GFR. Note on varying speed of light cosmologies. General Relativity and Gravitation. 2007;39(4):511–520. Available: <http://arxiv.org/abs/astro-ph/0703751>
19. Jovičević S. On vacuum dispersion and light velocity. Phys. Essays. 2005;18:518. Available: <http://physicsessays.org/browse-journal-2/pr...tml>
DOI: 10.4006/1.3025764
20. Von Weber S, von Eye A. Error analysis of simulated Einstein rings under the membrane paradigm. InterStat; 2013. Available: <http://interstat.statjournals.net/YEAR/2013/articles/1310001.pdf>
21. Everitt, et al. Gravity Probe B: Final results of a space experiment to test general relativity. PRL. 2011;106:221101. Available: https://einstein.stanford.edu/content/sci_papers/papers/PhysRevLett.106.221101.pdf
22. Bizouard MA, Papa MA. Searching for gravitational waves with the LIGO and Virgo interferometers. C. R. Physique. 2013;14:352-365. Available: [arXiv:1304.4984 \[gr-qc\]](https://arxiv.org/abs/1304.4984)
23. Magueijo J. New varying speed of light theories. Rept. Prog. Phys. 2003;66(11):2025. Available: <http://arxiv.org/abs/astro-ph/0305457>
24. Kaluza Th. Zum Unitätsproblem der Physik. Sitzungsberichte der Preussischen Akademie der Wissenschaften. 1921;96:69. Available: <http://homepage.uibk.ac.at/~c705204/pdf/kaluza-1921.pdf>
25. Müller E. De la réalité des nombres. Bull. Soc. Frib. Sc. Nat. 2014;103:83-90.
26. Ciufolini I. Dragging of inertial frames. Nature. 2007;449:41-47. Available: <http://www.nature.com/nature/journal/v449/n7158/abs/nature06071.html>
27. Conklin JW. For the gravity probe B collaboration, Stanford University: The gravity probe B experiment and early results, Sixth International Conference on gravitation and cosmology IOP publishing. Journal of Physics: Conference Series 140 012001; 2008. Available: <http://iopscience.iop.org/article/10.1088/1742-6596/140/1/012001/pdf>

© 2016 Weber and Eye; This is an Open Access article distributed under the terms of the Creative Commons Attribution License (<http://creativecommons.org/licenses/by/4.0>), which permits unrestricted use, distribution, and reproduction in any medium, provided the original work is properly cited.

Peer-review history:
The peer review history for this paper can be accessed here:
<http://sciencedomain.org/review-history/14928>